

Radiative capture of twisted electrons by bare ions

O Matula¹, A G Hayrapetyan¹, V G Serbo², A Surzhykov³ and S Fritzsche^{3,4}

¹Physikalisches Institut, Ruprecht-Karls-Universität Heidelberg, D-69120 Heidelberg, Germany

²Novosibirsk State University, RUS-630090 Novosibirsk, Russia

³Helmholtz-Institut Jena, D-07743 Jena, Germany

⁴Theoretisch-Physikalisches Institut, Friedrich-Schiller-Universität Jena, D-07743 Jena, Germany

E-mail: omatula@physi.uni-heidelberg.de

Received 30 January 2014, revised 18 March 2014

Accepted for publication 1 April 2014

Published 9 May 2014

New Journal of Physics **16** (2014) 053024

doi:[10.1088/1367-2630/16/5/053024](https://doi.org/10.1088/1367-2630/16/5/053024)

Abstract

Recent advances in the production of twisted electron beams with a sub-nanometer spot size offer unique opportunities to explore the role of orbital angular momentum in basic atomic processes. In the present work, we address one of these processes: radiative recombination of twisted electrons with bare ions. On the basis of the density matrix formalism and the non-relativistic Schrödinger theory, analytical expressions are derived for the angular distribution and the linear polarization of photons emitted due to the capture of twisted electrons into the ground state of (hydrogen-like) ions. We show that these angular and polarization distributions are sensitive to both the transverse momentum and the topological charge of the electron beam. To observe in particular the value of this charge, we propose an experiment that makes use of the coherent superposition of two twisted beams.

Keywords: radiative recombination, twisted electrons, angular distribution, polarization

1. Introduction

Beams of electrons that each carry a well-defined projection $\hbar m$ of orbital angular momentum (OAM) onto the propagation direction are currently attracting considerable interest in both



Content from this work may be used under the terms of the [Creative Commons Attribution 3.0 licence](https://creativecommons.org/licenses/by/3.0/). Any further distribution of this work must maintain attribution to the author(s) and the title of the work, journal citation and DOI.

fundamental and applied research [1–4]. These so-called *twisted* or *vortex* beams can be readily generated with a kinetic energy of up to a few hundred keV and with a topological charge m as high as $m=100$ [2–6]. Their unique features make these beams ideal tools for novel studies in various fields of modern physics. Scattering of twisted electrons on a solid target, for example, can provide detailed insights into the magnetic structure of the target materials [3, 7, 8]. When propagating in external (electric and magnetic) fields, beams with non-zero OAM help explore the vacuum Faraday effect [9], Larmor and Gouy rotations [10], or the formation of modified Landau and Aharonov–Bohm levels [11, 12]. Moreover, the production of electron vortex beams with a subnanometer focal spot size [5, 13] opens up new possibilities for investigating effects originating from the transfer of OAM in *electron–ion collisions*.

One fundamental process that takes place when electrons collide with matter is the capture of an electron into an atomic or ionic bound state accompanied by the emission of a photon [14]. Such a *radiative recombination* (RR), which can be viewed as the time-reversed photoionization, occurs frequently in stellar and laboratory plasmas as well as in ion trap and storage ring experiments. During the past few decades, therefore, this process has attracted much attention both in experiment and theory [15–17]. Even though these investigations have provided valuable knowledge on spin, relativistic, and quantum electrodynamic (QED) effects in the electron–photon coupling, they were restricted to the case of ‘standard’ plane-wave electron beams—beams without an OAM along the propagation axis.

Twisted electron beams offer a new and intriguing degree of freedom for the RR process: a *non-zero* orbital momentum $\hbar m$ along the propagation direction. To analyze how an OAM of the (free) electrons may influence the RR process and especially the properties of the emitted light, we use here the density matrix formalism based on the Schrödinger equation. Such a non-relativistic approach is well justified for (relatively) slow collisions with light ions and enables us to derive *analytical* expressions for the angular distribution and polarization of the recombination photons emitted in the capture of twisted electrons into the K shell of (finally) hydrogen-like ions, i.e. before the capture, no other bound electrons are present. On the basis of these expressions, we show that both the emission pattern and the linear polarization of the RR radiation may change significantly if a twisted instead of a plane-wave electron beam is used—modifications that can be easily measured with present-day detectors.

Hartree atomic units ($\hbar = e = m_e = 1$) are used throughout the paper.

2. Theoretical background

Photons emitted in the capture of electrons to an ionic bound state $|b\rangle$ are characterized by their energy, angular distribution and polarization. While the energy $E_\gamma = E_{\text{kin}} + |E_b|$ is uniquely defined by the velocity v of the incident electrons (and, hence, by $E_{\text{kin}} = v^2/2$) as well as the binding energy E_b , the angular and polarization properties of the RR radiation are sensitive to details of the electron–photon interaction. In atomic theory, one usually describes these properties via (i) the probability $W(\mathbf{k})$ of emitting a photon into a certain direction \mathbf{k}/k , \mathbf{k} being the wavevector, and (ii) the three Stokes parameters P_i , $i = 1, 2, 3$. The first two Stokes parameters quantify ‘relative’ asymmetries between intensities I_χ of light that is *linearly* polarized under different angles χ with respect to the reaction plane: $P_1 = (I_0 - I_{90})/(I_0 + I_{90})$

and $P_2 = (I_{45} - I_{135}) / (I_{45} + I_{135})$. Here the reaction plane is formed by the directions of the incident electron and the emitted photon. Moreover, the parameter P_3 reflects the degree of *circular* polarization of the emitted photons.

The emission probability $W(\mathbf{k})$ and the Stokes parameters P_i of the RR photons are described most conveniently within the density matrix framework [18, 19]. Using this formalism, the aforementioned quantities are directly related to the so-called photon spin density matrix (cf equation (1.106) in [18] taken with the normalization (1.11) therein):

$$\langle \mathbf{k}\lambda | \hat{\rho}_\gamma | \mathbf{k}\lambda' \rangle_{\lambda, \lambda' = \pm 1} = \frac{W(\mathbf{k})}{2} \begin{pmatrix} 1 + P_3 & -P_1 + iP_2 \\ -P_1 - iP_2 & 1 - P_3 \end{pmatrix}, \quad (1)$$

where $\lambda = \pm 1$ is the helicity of the emitted photon, i.e. its spin projection onto the direction of propagation.

2.1. Radiative recombination with plane-wave electrons

Before we derive the density matrix (1) for the capture of twisted electrons, let us briefly recall the recombination process for plane-wave electrons. By restricting ourselves to the RR of non-relativistic electrons into the 1 s ground state of bare ions with low nuclear charge Z , we can obtain the photon density matrix (1) as

$$\langle \mathbf{k}\lambda | \hat{\rho}_\gamma^{\text{pl}} | \mathbf{k}\lambda' \rangle = M_{\mathbf{k}, \mathbf{p}}^{\text{pl},*}(\lambda) M_{\mathbf{k}, \mathbf{p}}^{\text{pl}}(\lambda'), \quad (2)$$

where the (transition) amplitude

$$M_{\mathbf{k}, \mathbf{p}}^{\text{pl}}(\lambda) = \int \psi_f^*(\mathbf{r}) e^{-i\mathbf{k}\cdot\mathbf{r}} (\mathbf{e}_\lambda^* \cdot \hat{\mathbf{p}}) \psi_i^{\text{pl}}(\mathbf{r}) d^3\mathbf{r} \quad (3)$$

describes the emission of a photon with polarization \mathbf{e}_λ and wavevector \mathbf{k} . In this process, moreover, the electron performs a transition from the (initial) continuum state $\psi_i^{\text{pl}}(\mathbf{r}) \equiv \psi_{\mathbf{p}}^{\text{pl}}(\mathbf{r})$ with momentum \mathbf{p} into the (final) ionic ground state $\psi_f(\mathbf{r}) = \psi_{1s}(\mathbf{r}) \equiv \sqrt{Z^3/\pi} e^{-Zr}$, and couples to the photon via the momentum operator $\hat{\mathbf{p}} = -i\partial/\partial\mathbf{r}$. The amplitude (3) can be evaluated analytically to give [20, 21]

$$M_{\mathbf{k}, \mathbf{p}}^{\text{pl}}(\lambda) = 8\sqrt{\pi Z^5} \frac{(\mathbf{e}_\lambda^* \cdot \mathbf{p})}{\left[(\mathbf{p} - \mathbf{k})^2 + Z^2 \right]^2} \quad (4)$$

if the incoming electron is *approximated* as a plane wave $\psi_i^{\text{pl}}(\mathbf{r}) = e^{i\mathbf{p}\cdot\mathbf{r}}$. Although the plane-wave approximation neglects the (Coulomb) interaction of the incoming electron with the ion before the capture process, it is well justified to describe the (angle-differential) properties of the emitted photons for kinetic energies E_{kin} of the electrons that are much higher than the ionization threshold of the 1 s ground state but still non-relativistic (and thus lower than the electron rest energy): $|E_{1s}| \ll E_{\text{kin}} \ll m_e c^2$ [20, 21]. Since in the present study we focus on energetic (but still non-relativistic) collisions, we will use equation (4) in the calculations below. Such energetic collisions are easily realizable with present-day electron beam ion trap and storage ring facilities and allow us to study the RR process for electrons with typical (kinetic)

energies of a few keV up to several hundred keV (corresponding to velocities from approximately 5% to 85% of the speed of light) [14, 22–24]. Moreover, recent advances in electron cooling techniques allow us to extend such studies to electron energies of only a few eV [25, 26].

Inserting the transition amplitude (4) into equations (1)–(2) leads (after some simple algebra) to the ‘standard’ expressions for the angular distribution and polarization of the RR radiation that follows the capture of plane-wave electrons into the ground state of a (hydrogen-like) ion [20, 21]. More specifically, the emitted photons are completely linearly polarized within the reaction plane (as given by the directions of the incoming electron and the emitted photon),

$$P_1 = 1,$$

and their emission pattern reads

$$W(\mathbf{k}) \propto \sin^2\theta_k / [p^2 + k^2 + Z^2 - 2pk \cos\theta_k]^4,$$

where θ_k denotes the polar angle of the wavevector \mathbf{k} with regard to the direction of the incident electron beam. Furthermore, by comparing the angular distribution as well as the polarization of the RR photons with results obtained from (exact) calculations performed with Coulomb-distorted wavefunctions [27–29], we ascertain that the relative deviations with respect to the exact calculations amount to less than 2% within the energy regime $100 \text{ eV} \leq E_{\text{kin}} \leq 50 \text{ keV}$ and, hence, we confirm that in this regime the plane-wave approximation used in equations (3)–(4) is accurate.

2.2. Radiative recombination with twisted electrons

To explore how a twisted electron beam affects the angular and polarization properties of the recombination light, we return to the general expression (1) for the photon spin density matrix. Like for the capture of plane-wave electrons, the evaluation of this matrix is traced back to the RR amplitudes and, hence, to the explicit form of the electron wavefunctions. While the final (bound) state is again described by the function $\psi_f(\mathbf{r}) = \psi_{1s}(\mathbf{r})$, the initial wavefunction $\psi_i(\mathbf{r})$ should be modified to represent a twisted electron state. Following recent studies [12, 30, 31], we assume here that the electrons are prepared as a (twisted) *wave packet* with well-defined values of (i) the linear momentum p_z and (ii) the OAM $m = 0, \pm 1, \pm 2, \dots$ along the propagation direction, which is taken as the quantization z -axis. In this case, the initial-state wavefunction reads

$$\psi_i^{\text{tw}}(\mathbf{r}) \equiv \psi_{xmp_z}^{\text{tw}}(\mathbf{r}) = \int a_{xm}(\mathbf{p}_\perp) e^{i(\mathbf{p}_\perp \cdot \mathbf{r}_\perp + p_z z)} \frac{d^2 \mathbf{p}_\perp}{(2\pi)^2}, \quad (5)$$

where the (Fourier) coefficient a_{xm} is

$$a_{xm}(\mathbf{p}_\perp) = \sqrt{\frac{2\pi}{p_\perp}} (-i)^m e^{im\varphi_p} g_x(p_\perp), \quad (6)$$

and the function $g_x(p_\perp)$ describes the transverse momentum profile of the beam. We suppose here a Gaussian function $g_x(p_\perp) = (\pi\sigma_x^2)^{-1/4} e^{-(p_\perp - x)^2/(2\sigma_x^2)}$ with a width $\sigma_x \ll x$. This implies that

the wave packet (5) has a mean kinetic energy $E_{\text{kin}} = (\chi^2 + p_z^2)/2$ and that its momentum distribution peaks sharply at $p_\perp = \chi$.

The twisted electron wave (5)–(6) can be considered as a coherent superposition of (tilted) plane waves $e^{i\mathbf{p}\cdot\mathbf{r}} = e^{i(p_\perp r_\perp + p_z z)}$ whose momentum vectors \mathbf{p} form the surface of a cone with (mean) opening angle $\theta_p = \arctan(\chi/p_z)$. As known from the literature [12, 30–32], it is the azimuthal phase factor $\exp(im\varphi_p)$ of the superposition coefficients (6) that gives rise to the well-defined (projection of) OAM $\hbar m$ and leads also to a pronounced *spatial* profile of the electron packet. That is, the electron probability density exhibits for $m \neq 0$ a concentric ring structure with a central dark spot within a plane perpendicular to the z - (propagation) axis.

Owing to the complex spatial structure of the state (5), the properties of the emitted photons depend on the *position* of a target ion within the electron wavefront. This is taken into account by translating the final-state wavefunction

$$\psi_f(\mathbf{r} - \mathbf{b}_\perp) = e^{-i\hat{\mathbf{p}}\cdot\mathbf{b}_\perp}\psi_f(\mathbf{r}) \quad (7)$$

from the (zero-intensity) center of the electron wave by a (transverse) vector \mathbf{b}_\perp . Employing expression (7) and the initial-state wavefunction (5), we finally obtain the amplitude

$$\begin{aligned} M_{\mathbf{k},\chi,p_z,\mathbf{b}_\perp}^{\text{tw}}(\lambda) &= \int \psi_f^*(\mathbf{r} - \mathbf{b}_\perp) e^{-i\mathbf{k}\cdot\mathbf{r}} (\mathbf{e}_\lambda^* \cdot \hat{\mathbf{p}}) \psi_i^{\text{tw}}(\mathbf{r}) d^3\mathbf{r} \\ &= \int e^{i(p_\perp - k_\perp)\cdot\mathbf{b}_\perp} a_{\chi m}(\mathbf{p}_\perp) M_{\mathbf{k},\mathbf{p}}^{\text{pl}}(\lambda) \frac{d^2\mathbf{p}_\perp}{(2\pi)^2} \end{aligned} \quad (8)$$

that describes the capture of a twisted electron by an ion with impact parameter \mathbf{b}_\perp . As seen from the second line of equation (8), such an amplitude can be represented in terms of the standard ‘plane-wave’ matrix elements (4). We can simplify equation (8) further by taking into account that the transverse momentum distribution $g_\chi(p_\perp)$ within the coefficients $a_{\chi m}(\mathbf{p}_\perp)$ (cf equation (6)) is sharply peaked at the value $p_\perp = \chi$ with a width $\sigma_\chi \ll \chi$, so we may write

$$M_{\mathbf{k},\chi,p_z,\mathbf{b}_\perp}^{\text{tw}}(\lambda) \approx C_{\chi,\sigma_\chi} \int (-i)^m e^{im\varphi_p} e^{i(p_\perp - k_\perp)\cdot\mathbf{b}_\perp} M_{\mathbf{k},\mathbf{p}}^{\text{pl}}(\lambda) \left. \frac{d\varphi_p}{(2\pi)^2} \right|_{p_\perp=\chi} \quad (9)$$

with

$$\begin{aligned} C_{\chi,\sigma_\chi} &= \sqrt{2\pi} \int g_\chi(p_\perp) \sqrt{p_\perp} dp_\perp = \frac{\pi^2 \chi^{3/2}}{2\sqrt{2} \sigma_\chi^{1/2}} \exp\left[-\chi^2/(4\sigma_\chi^2)\right] \\ &\times \left[I_{-1/4}\left(\frac{\chi^2}{4\sigma_\chi^2}\right) + (1 + 2\sigma_\chi^2/\chi^2) I_{1/4}\left(\frac{\chi^2}{4\sigma_\chi^2}\right) + I_{3/4}\left(\frac{\chi^2}{4\sigma_\chi^2}\right) + I_{5/4}\left(\frac{\chi^2}{4\sigma_\chi^2}\right) \right], \end{aligned} \quad (10)$$

where the $I_n(x)$ denote modified Bessel functions of the first kind [33].

The amplitudes (9) provide the main building blocks for constructing the photon density matrix for K-shell RR of twisted electrons. Beside the amplitudes, however, this matrix depends also on the setup of a particular ‘experiment’. Typically, the twisted electrons collide with some macroscopic ion target and, hence, no information is available about the impact parameter \mathbf{b}_\perp .

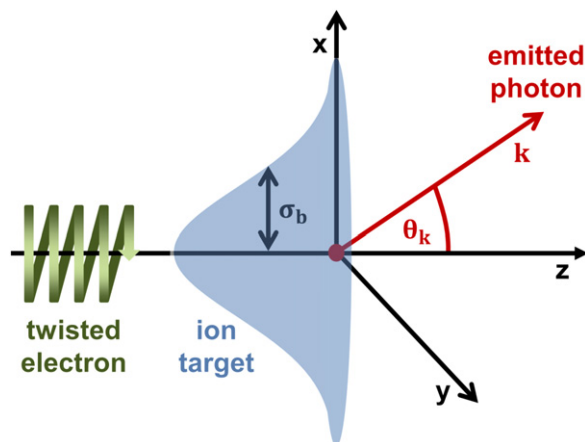


Figure 1. Geometry for the radiative capture of twisted electrons by bare ions. The (quantization) z -axis is chosen along the propagation direction of the electron wave. The recombination photon is emitted under a polar angle θ_k . Its momentum \mathbf{k} defines, together with the z -axis, the x - z -plane.

The photon density matrix then reads

$$\langle \mathbf{k}\lambda | \hat{\rho}_\gamma^{\text{tw}} | \mathbf{k}\lambda' \rangle = \int f(\mathbf{b}_\perp) M_{\mathbf{k},x,p_z,\mathbf{b}_\perp}^{\text{tw},*}(\lambda) M_{\mathbf{k},x,p_z,\mathbf{b}_\perp}^{\text{tw}}(\lambda') d^2\mathbf{b}_\perp, \quad (11)$$

where $f(\mathbf{b}_\perp)$ denotes the probability of finding a target ion at a (transverse) position \mathbf{b}_\perp with respect to the center of the incident electron beam. By choosing a Gaussian function $f(\mathbf{b}_\perp) = (2\pi\sigma_b^2)^{-1} e^{-\mathbf{b}_\perp^2/(2\sigma_b^2)}$ with a width σ_b for the distribution of the ions—cf figure 1—and by making use of equation (9), we find

$$\begin{aligned} \langle \mathbf{k}\lambda | \hat{\rho}_\gamma^{\text{tw}} | \mathbf{k}\lambda' \rangle &= C_{\chi,\sigma_x}^2 \int \exp \left[-2\chi^2 \sigma_b^2 \sin^2 \left(\frac{\varphi_p - \varphi'_p}{2} \right) \right] \\ &\times e^{im(\varphi'_p - \varphi_p)} M_{\mathbf{k},\mathbf{p}}^{\text{pl},*}(\lambda) M_{\mathbf{k},\mathbf{p}}^{\text{pl}}(\lambda') \frac{d\varphi_p}{(2\pi)^2} \frac{d\varphi'_p}{(2\pi)^2} \end{aligned} \quad (12)$$

after integrating over the impact parameter \mathbf{b}_\perp .

If—as usual in collision experiments—the width of the incoming electron beam is considerably smaller than the size of the ionic target and, hence, $1/\sigma_x \ll \sigma_b$, the density matrix can be evaluated analytically. In this case the exponent in equation (12) acts (up to some factor) as a delta distribution $\delta(\varphi_p - \varphi'_p)$, thus allowing us to write

$$\langle \mathbf{k}\lambda | \hat{\rho}_\gamma^{\text{tw}} | \mathbf{k}\lambda' \rangle \propto \int M_{\mathbf{k},\mathbf{p}}^{\text{pl},*}(\lambda) M_{\mathbf{k},\mathbf{p}}^{\text{pl}}(\lambda') d\varphi_p. \quad (13)$$

As seen from equation (13), on using a *macroscopic* ion target that is much larger than the twisted electron beam, the photon spin density matrix becomes independent of the topological charge m of the beam. However, this matrix still reflects the (conic) momentum structure of the electron beam, that is, it still contains the φ_p -integration that originates from the composition of the twisted electron wave into (tilted) plane waves (see equations (5)–(6) and the subsequent

discussion). Employing the transition amplitudes (3) for the RR process with plane-wave electrons allows us to evaluate the remaining integration over φ_p in equation (13) as

$$\left\langle \mathbf{k}\lambda \left| \hat{\rho}_\gamma^{\text{tw}} \right| \mathbf{k}\lambda' \right\rangle \propto Q_1(\mathbf{k}) + \lambda\lambda' Q_2(\mathbf{k}). \quad (14)$$

The functions Q_1 and Q_2 do not depend on the polarization (helicity) states of the emitted radiation and can be expressed solely in terms of kinematic parameters such as the opening angle θ_p and the momentum $p = \sqrt{x^2 + p_z^2}$ of the twisted electron packet as well as the wavevector \mathbf{k} of the photon:

$$Q_1(\mathbf{k}) = \frac{1}{4v^4(1-u^2)^{7/2}} (1-u^2) \sin^2\theta_p, \quad (15)$$

$$Q_2(\mathbf{k}) = \frac{1}{8v^4(1-u^2)^{7/2}} \left[2(2+3u^2) \sin^2\theta_k \cos^2\theta_p - (4u+u^3) \sin 2\theta_k \sin 2\theta_p \right. \\ \left. + 2(1+4u^2) \cos^2\theta_k \sin^2\theta_p \right], \quad (16)$$

where the notation

$$u = \frac{2pk}{v} \sin\theta_p \sin\theta_k, \quad 0 \leq u < 1, \quad (17)$$

$$v = p^2 + k^2 + Z^2 - 2pk \cos\theta_p \cos\theta_k, \quad 0 < v, \quad (18)$$

is used and the emission angle θ_k is defined with respect to the incident beam direction (cf figure 1).

By employing the photon spin density matrix (14) and equation (1), one can study the angular and polarization properties of recombination photons for an (incident) twisted electron beam. For example, if we take the trace of (14) over the photon helicities, we immediately find

$$W(\mathbf{k}) = \sum_\lambda \left\langle \mathbf{k}\lambda \left| \hat{\rho}_\gamma^{\text{tw}} \right| \mathbf{k}\lambda \right\rangle = \mathcal{N}(Q_1(\mathbf{k}) + Q_2(\mathbf{k})), \quad (19)$$

where $\mathcal{N} = 3 \left[(p^2 - k^2)^2 + 2Z^2(p^2 + k^2) + Z^4 \right]^2$ is defined from the normalization condition $\int W(\mathbf{k}) d\Omega_k = 4\pi$. The polarization of the RR radiation is characterized, moreover, by the single Stokes parameter

$$P_1 = \frac{Q_2(\mathbf{k}) - Q_1(\mathbf{k})}{Q_1(\mathbf{k}) + Q_2(\mathbf{k})}, \quad (20)$$

while P_2 and P_3 vanish identically.

2.3. Radiative recombination with twisted electrons: paraxial regime

Equations (19) and (20) describe the emission pattern and the Stokes parameter P_1 of the RR radiation for the twisted electron waves (5) with any arbitrary ratio of the transverse and longitudinal momenta x and p_z . Most studies in the past, however, have dealt with *paraxial*

beams, characterized by small ratios $\kappa/p_z \ll 1$ and, hence, opening angles $\theta_p \lesssim 1^\circ$ [2–6]. For such beams, equations (15)–(20) can be further simplified to give

$$W(\mathbf{k}) \simeq \frac{\mathcal{N}}{2} \frac{\sin^2\theta_k + \sin^2\theta_p P_2(\cos\theta_k)}{(p^2 + k^2 + Z^2 - 2pk \cos\theta_k)^4}, \quad (21)$$

$$P_1 \simeq 1 - \frac{\sin^2\theta_p}{\sin^2\theta_k + \sin^2\theta_p P_2(\cos\theta_k)}, \quad (22)$$

where $P_2(\cos\theta_k) = (3\cos^2\theta_k - 1)/2$ denotes the second-order Legendre polynomial. As seen from these formulas, both the angular distribution and the linear polarization of the emitted photons are described by a sum of the ‘standard’ expression, as obtained for the plane-wave electrons, *and* an additional term proportional to $\sin^2\theta_p$. This latter term arises due to the transverse momentum of the incident electron and, hence, disappears when this momentum turns to zero, $\kappa \rightarrow 0$, or equivalently $\theta_p \rightarrow 0$.

3. Results and discussion

Both the general and the approximate expressions (19)–(22) for the angular distribution and linear polarization of the RR photons were derived for twisted electron beams whose width, $\sim 1/\sigma_x$, is much smaller compared to the size of a *macroscopic* target σ_b . For such a scenario, which can be easily realized experimentally, the properties of the emitted photons are insensitive to the topological charge m and depend only on the (mean) transverse momentum κ of the electron packet as characterized by the angle θ_p . In figure 2 we display the angular distribution (left panel) and the Stokes parameter P_1 (right panel) as resulting for the radiative capture of twisted electrons with $E_{\text{kin}} = 2$ keV into the ground state of (finally) hydrogen atoms, and for different opening angles θ_p .

As expected already from equations (21)–(22), both (angular and polarization) properties resemble the ‘plane-wave’ behavior $W(\mathbf{k}) \sim \sin^2\theta_k$ and $P_1 \sim 1$ in the *paraxial* regime where $\theta_p \lesssim 1^\circ$. However, a strong enhancement of the RR-photon yield can be observed in the forward ($\theta_k \lesssim 30^\circ$) and backward ($\theta_k \gtrsim 150^\circ$) directions with respect to the incident electron beam as the opening angle is increased. At these emission angles, moreover, the Stokes parameter P_1 drops by factors of 1.5 to 10 if θ_p changes from 1° to 45° . By employing modern detectors, such a modification of the polarization (as well as of the angular distribution) can be easily observed, and thus these measurements may be used to further explore the interaction of twisted electrons with matter.

Until now, we have discussed the capture of twisted electrons that are prepared in a pure state with well-defined OAM $\hbar m$. As mentioned already, in such a case the angular and polarization properties of the emitted light are sensitive to the opening angle θ_p , but not to the topological charge m of the beam. This insensitivity can be overcome if the incident electron packet is prepared as a coherent superposition of two states with different projections m_1 and m_2 of orbital momentum onto the mutual propagation z -axis [10, 34]:

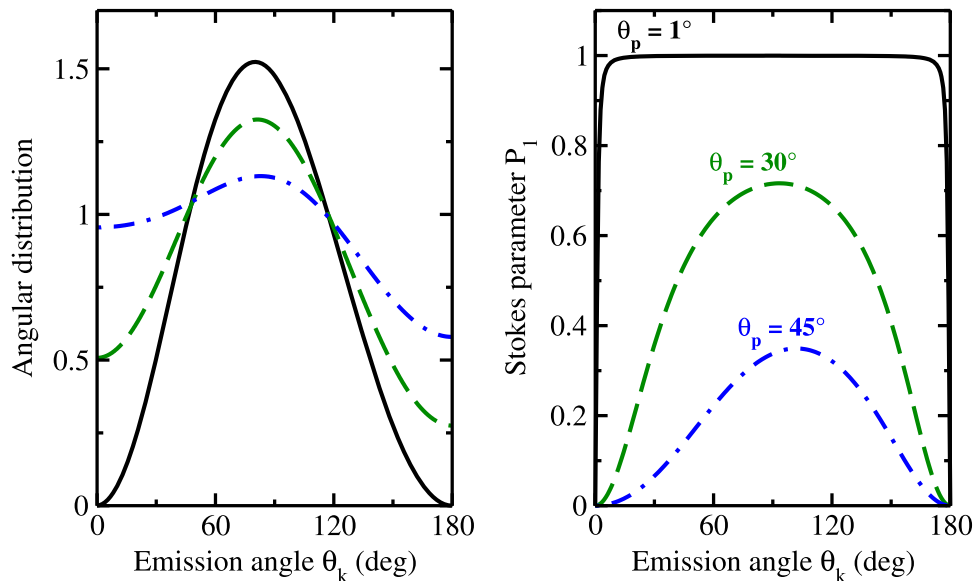


Figure 2. Angular distribution (left panel) and Stokes parameter P_1 (right panel) of photons emitted in the capture of twisted electrons into the 1s ground state of a hydrogen atom. The calculations, based on equations (19) and (20), were performed for an electron beam with an energy of $E_{\text{kin}} = 2$ keV and for three different values of the opening angle: $\theta_p = 1^\circ$ (black solid lines), $\theta_p = 30^\circ$ (green dashed lines) and $\theta_p = 45^\circ$ (blue dashed–dotted lines).

$$\psi_i^{\text{tw}}(\mathbf{r}) = c_1 \psi_{\chi m_1 p_z}^{\text{tw}}(\mathbf{r}) + c_2 e^{i\zeta} \psi_{\chi m_2 p_z}^{\text{tw}}(\mathbf{r}), \quad (23)$$

where c_1 and c_2 are (real) weight factors with $|c_1|^2 + |c_2|^2 = 1$ and ζ is a relative phase. Inserting this formula into equations (8)–(11), the photon density matrix

$$\langle \mathbf{k}\lambda \left| \hat{\rho}_\gamma^{\text{tw}} \right| \mathbf{k}\lambda' \rangle \propto \int_0^{2\pi} \left\{ 1 + 2|c_1 c_2| \cos \left[\Delta m \left(\varphi_p - \pi/2 \right) + \zeta \right] \right\} M_{\mathbf{k},\mathbf{p}}^{\text{pl},*}(\lambda) M_{\mathbf{k},\mathbf{p}}^{\text{pl}}(\lambda') d\varphi_p \quad (24)$$

can be written as a sum of the matrix (14) that was obtained for the individual electron beams and an interference term that depends on the difference $\Delta m = m_2 - m_1$. Such a Δm -dependence translates directly to the properties of the emitted light. As seen from figure 3, for example, both the angular distribution and the polarization P_1 are strongly affected by the variation of Δm if the electron packets are prepared in a state with energy $E_{\text{kin}} = 2$ keV, opening angle $\theta_p = 45^\circ$, and OAM $m_1 = 0$ and $m_2 = 0, \pm 1$.

Moreover, the second Stokes parameter P_2 , which is identically zero for a single wave packet (5) with a well-defined m , becomes considerably larger if $\Delta m \neq 0$ (cf right panel of figure 3). We therefore conclude that the Δm -dependence enables one to *determine* the OAM of an electron packet when it is mixed coherently with a ‘reference’ beam whose topological charge m is well known.

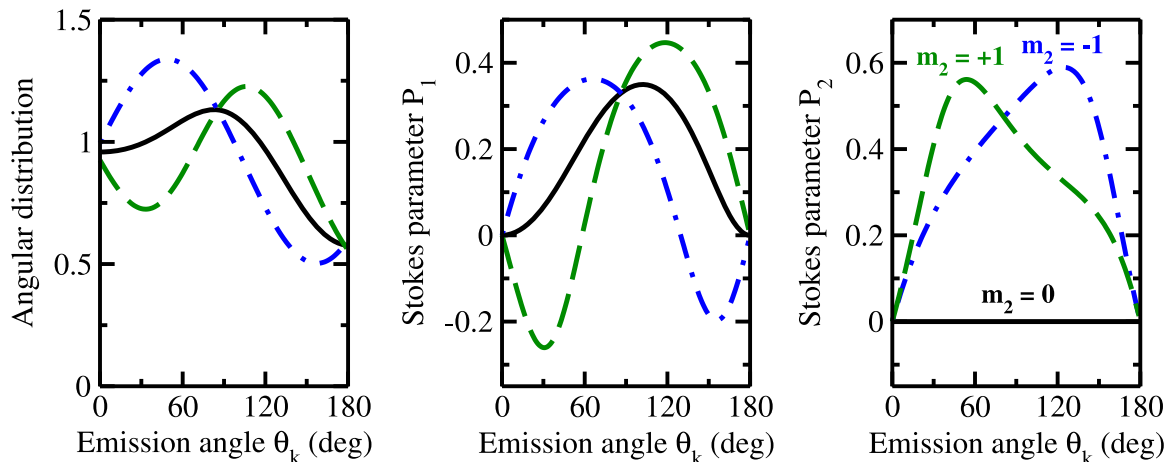


Figure 3. Angular distribution (left panel) and Stokes parameters P_1 (middle panel) and P_2 (right panel) of photons emitted in the capture of twisted electrons into the $1s$ ground state of a hydrogen atom. Here the electrons are in a superposition of two states with relative phase $\zeta = \pi/4$ and projections of the OAM $m_1 = 0$, and $m_2 = 0$ (black solid lines), $m_2 = +1$ (green dashed lines) or $m_2 = -1$ (blue dashed-dotted lines), respectively. For $m_1 = m_2 = 0$, this corresponds to a beam in the pure state with zero OAM. Results are shown for an electron energy $E_{\text{kin}} = 2$ keV and within the non-paraxial regime $\theta_p = 45^\circ$.

4. Conclusions

In summary, we have performed a theoretical study of the radiative recombination of twisted electrons with low- Z bare ions. On the basis of solutions of the non-relativistic Schrödinger equation for the capture into the ionic ground state, analytical expressions were derived for (i) the angular distribution and (ii) the Stokes parameters of the emitted photons. Depending on the particular setup of the recombination experiment, these (angular and polarization) properties appear to be sensitive to the kinematic parameters such as the ratio κ/p_z of transverse to longitudinal momentum as well as to the ‘twistedness’ of the incident electron beam. We argue, therefore, that observation of the K-shell radiative recombination of twisted electrons will provide additional details about the fundamental light–matter interaction process.

Acknowledgements

OM and AS acknowledge support from the Helmholtz Gemeinschaft and GSI (Nachwuchsgruppe VH-NG-421). AGH acknowledges support from the GSI Helmholtzzentrum and the University of Heidelberg. VGS is supported by the Russian Foundation for Basic Research via grants 13-02-00695 and NSh-3802.2012.2.

References

- [1] Bliokh K Y, Bliokh Y P, Savel’ev S and Nori F 2007 *Phys. Rev. Lett.* **99** 190404

- [2] Uchida M and Tonomura A 2010 *Nature* **464** 737
- [3] Verbeeck J, Tian H and Schattschneider P 2010 *Nature* **467** 301
- [4] McMorran B J *et al* 2011 *Science* **331** 192
- [5] Verbeeck J, Tian H and Béch e A 2012 *Ultramicroscopy* **113** 83
- [6] Saitoh K, Hasegawa Y, Tanaka N and Uchida M 2012 *J. Electron Microsc.* **61** 171
- [7] Lloyd S, Babiker M and Yuan J 2012 *Phys. Rev. Lett.* **108** 074802
- [8] Saitoh K, Hasegawa Y, Hirakawa K, Tanaka N and Uchida M 2013 *Phys. Rev. Lett.* **111** 074801
- [9] Greenshields C, Stamps R L and Franke-Arnold S 2012 *New J. Phys.* **14** 103040
- [10] Guzzinati G, Schattschneider P, Bliokh K Y, Nori F and Verbeeck J 2013 *Phys. Rev. Lett.* **110** 093601
- [11] Gallatin G M and McMorran B 2012 *Phys. Rev. A* **86** 012701
- [12] Bliokh K Y, Schattschneider P, Verbeeck J and Nori F 2012 *Phys. Rev. X* **2** 041011
- [13] Verbeeck J, Schattschneider P, Lazar S, St oger-Pollach M, L offler S, Steiger-Thirsfeld A and van Tendeloo G 2011 *Appl. Phys. Lett.* **99** 203109
- [14] Eichler J and St ohlker Th 2007 *Phys. Rep.* **439** 1
- [15] Scofield J H 1989 *Phys. Rev. A* **40** 3054
- [16] St ohlker Th *et al* 1995 *Phys. Rev. A* **51** 2098
- [17] Tashenov S *et al* 2006 *Phys. Rev. Lett.* **97** 223202
- [18] Balashov V V, Grum-Grzhimailo A N and Kabachnik N M 2000 *Polarization and Correlation Phenomena in Atomic Collisions* (New York: Kluwer)
- [19] Blum K 1981 *Density Matrix Theory and Applications* (New York: Plenum)
- [20] Bransden B H and Joachain C J 2003 *Physics of Atoms and Molecules* (Harlow: Pearson)
- [21] Bethe H A and Salpeter E E 1957 *Quantum Mechanics of One- and Two-Electron Atoms* (Berlin: Springer)
- [22] Hughes R H, Stigers C A, Doughty B M and Stokes E D 1970 *Phys. Rev. A* **1** 1424
- [23] Hughes R H, Stokes E D, Choe S S and King T J 1971 *Phys. Rev. A* **4** 1453
- [24] Biedermann C, Radtke R, Seidel R and Behar E 2009 *J. Phys.: Conf. Ser.* **163** 012034
- [25] Spies W *et al* 1992 *Phys. Rev. Lett.* **69** 2768
- [26] Uwira O *et al* 1997 *Hyperfine Interact.* **108** 149
- [27] Ichihara A and Eichler J 2000 *At. Data Nucl. Data Tables* **74** 1
- [28] Ichihara A and Eichler J 2001 *At. Data Nucl. Data Tables* **79** 187
- [29] Surzhykov A, Fritzsche S, St ohlker Th and Tachenov S 2003 *Phys. Rev. A* **68** 022710
- [30] Ivanov I P and Serbo V G 2011 *Phys. Rev. A* **84** 033804
- [31] Schattschneider P and Verbeeck J 2011 *Ultramicroscopy* **111** 1461
- [32] Matula O, Hayrapetyan A G, Serbo V G, Surzhykov A and Fritzsche S 2013 *J. Phys. B: At. Mol. Opt. Phys.* **46** 205002
- [33] Abramowitz M and Stegun I A 1970 *Handbook of Mathematical Functions* (New York: Dover)
- [34] Ivanov I P 2012 *Phys. Rev. A* **85** 033813